

APPLICATION OF A DOMAIN DECOMPOSITION TECHNIQUE TO THE MATHEMATICAL MODELLING OF A UTILITY BOILER

P. J. COELHO AND M. G. CARVALHO

*Instituto Superior Técnico, Technical University of Lisbon, Mechanical Engineering Department, Av. Rovisco Pais, 1096
Lisboa Codex, Portugal*

SUMMARY

Domain decomposition techniques are very effective for flow simulation, especially in domains where geometrical length scales of different orders of magnitude are present. In this work a zonal method is applied to the mathematical modelling of a power station boiler of the Portuguese Electricity Utility. The mathematical model is based on the numerical solution of the partial differential equations governing conservation of mass, momentum and energy. The zonal method is presented and the conservative treatment of the interfaces is described in detail. Emphasis is placed on the evaluation of the zonal method. The results show that the influence of the zonal method on the convergence rate of the solution algorithm is negligible. The zonal method does not influence the accuracy of the predicted results and there is continuity of the dependent variables across the interfaces. A significant reduction in CPU time is feasible due to a better distribution of grid nodes and consequent reduction in the total number of grid nodes required.

1. INTRODUCTION

The use of CFD codes for modelling utility boilers is becoming a widespread tool among the scientific and industrial communities. It helps engineers to optimize the operating conditions, reduce pollutants emission, investigate malfunctions in the equipment and evaluate different corrective measures. It can also improve the design of new boilers.

Among the mathematical models available, those based on the numerical solution of the equations governing conservation of mass, momentum and energy are the most powerful.¹⁻⁶ They simulate all the relevant physical phenomena occurring in the combustion chamber of a utility boiler: turbulent three-dimensional flow, combustion, heat and mass transfer. However, the computational requirements involved are very high. Therefore, the numerical grids employed are often too coarse, yielding grid-dependent solutions.

This problem was investigated by Gillis and Smith.⁷ They pointed out that previous related studies published in the literature have used grids that were too coarse. Their calculations for non-reactive flows show that in wall-fired boilers, grids much finer than those previously employed are required to achieve grid-independent solutions. The number of grid nodes required would be much higher for coal-fired or fuel-oil-fired boilers. In this case, the presence of geometrical length scales of different orders of magnitude prevents the accurate simulation of the near burners region when a single grid is used. For example, the overall dimensions of fuel-oil-fired boilers are three to four orders of magnitude higher than the characteristic dimensions of the atomizers. Hence, a grid adequate for flow simulation in the small length scales regions would be prohibitively expensive as far as computational requirements are concerned. To avoid this

problem, it would be highly advantageous if grid refinement could be restricted according to the local length scales. This can be accomplished using a domain decomposition technique.

Domain decomposition techniques were introduced many years ago for solving differential equations. However, their application in CFD is much more recent. Nowadays, they are widely employed in aeronautics and turbomachinery for the simulation of compressible flows. Zonal methods^{8,9} are among the more popular domain decomposition techniques. The physical domain is divided into a number of subdomains and different grids are used for each of them. The differential equations are then solved for each subdomain sweeping iteratively all the subdomains until the iteration process converges.

Although zonal methods are very common in the calculation of compressible flows, their application to the simulation of incompressible flows is rather limited. In some applications of zonal methods to the calculation of incompressible flows, the grids generated for each block are continuous across the interblock boundaries.^{10,11} In this case, although it remains feasible to deal with complex geometries, it is not possible to use different levels of grid refinement in different zones. Therefore, this implementation of zonal methods is not suitable for our purpose. To allow local grid refinement, it is necessary to have discontinuous grids across the interblock boundaries (see References 12 and 13).

Calculation of incompressible reactive flows using zonal methods has seldom been attempted. Wild *et al.*¹⁴ have employed two zones in the mathematical modelling of a gas turbine combustion chamber but no details about the treatment of the interfaces are given. Recently, Rachner¹⁵ applied a zonal method to flow modelling in an axisymmetric combustion chamber and to a single crossflow jet in a rectangular channel. Zhu and Rodi¹⁶ calculated several laminar elliptic flows using non-orthogonal and non-staggered grids and a zonal method with grid continuity along the interfaces. None of these studies have considered the radiative heat transfer which plays a dominant role in utility boilers. It should be mentioned that several authors have used two or more subdomains in the mathematical modelling of industrial furnaces.¹⁷⁻²¹ However, the calculations in each zone were performed until convergence, and each subdomain was visited at most three times. Therefore, coupling between the different zones is very weak and the applicability of this methodology is limited.

The objective of this paper is the application of a zonal method to the mathematical modelling of a utility boiler using a full three-dimensional model. Grids for different zones are independent and discontinuous across the interfaces between different zones. A conservative procedure to transfer data between adjacent zones is employed. Emphasis is placed on the validation of the zonal method. Evaluation of the physical models is not made here. There are some measurements available and the predicted results are in reasonable agreement with them.²²

The mathematical and physical models are described in the following section. Then, the numerical model and the zonal method are described in detail. The computations performed to validate the method are presented in Section 4. The paper concludes with an evaluation of the zonal method and its ability to overcome the problem of length scales of different orders of magnitude.

2. MATHEMATICAL AND PHYSICAL MODELS

The governing Favre-averaged conservation equations for a turbulent high-Reynolds number flow can be written in Cartesian co-ordinates as follows (see, e.g. Reference 23) :

Continuity

$$\frac{\partial}{\partial x_i}(\bar{\rho} \tilde{u}_i) = 0 \quad (1)$$

Momentum

$$\frac{\partial(\bar{\rho}\tilde{u}_i\tilde{u}_j)}{\partial x_j} = -\frac{\partial}{\partial x_j}(\bar{\rho}\tilde{u}_i''\tilde{u}_j'') - \frac{\partial\bar{p}}{\partial x_i} \quad (2)$$

Scalar

$$\frac{\partial(\bar{\rho}\tilde{u}_j\tilde{\phi})}{\partial x_j} = -\frac{\partial}{\partial x_j}(\bar{\rho}\tilde{u}_j''\tilde{\phi}'') + \bar{\rho}\tilde{S}_\phi \quad (3)$$

where $\tilde{\phi}$ stands for scalar properties such as mixture fraction or stagnation enthalpy and \tilde{S}_ϕ denotes a source/sink of a scalar quantity. Superscripts $\bar{\cdot}$, $\tilde{\cdot}$ and $''$ identify Reynolds-average values, Favre-average values and fluctuation quantities in Favre-averaging, respectively.

The turbulence model

The mean-flow equations are closed by the k - ε eddy viscosity/diffusivity model which comprises transport equations for the turbulent kinetic energy, k , its dissipation rate, ε , and constitutive relations for the Reynolds stresses $\tilde{u}_i''\tilde{u}_j''$ and turbulent scalar fluxes $\tilde{u}_j''\tilde{\phi}''$:

$$-\bar{\rho}\tilde{u}_i''\tilde{u}_j'' = \mu_t \left(\frac{\partial\tilde{u}_i}{\partial x_j} + \frac{\partial\tilde{u}_j}{\partial x_i} \right) - \frac{2}{3} \left(\bar{\rho}k + \mu_t \frac{\partial\tilde{u}_k}{\partial x_k} \right) \delta_{ij} \quad (4)$$

$$-\bar{\rho}\tilde{u}_j''\tilde{\phi}'' = \frac{\mu_t}{\sigma_\phi} \frac{\partial\tilde{\phi}}{\partial x_j} \quad (5)$$

$$\frac{\partial}{\partial x_j}(\bar{\rho}\tilde{u}_j k) = \frac{\partial}{\partial x_j} \left[\left(\frac{\mu_t}{\sigma_k} + \mu \right) \frac{\partial k}{\partial x_j} \right] + G - \bar{\rho}\varepsilon - \frac{\mu_t}{\bar{\rho}^2} \frac{\partial\bar{\rho}}{\partial x_j} \frac{\partial\bar{p}}{\partial x_j} \quad (6)$$

$$\frac{\partial}{\partial x_j}(\bar{\rho}\tilde{u}_j\varepsilon) = \frac{\partial}{\partial x_j} \left[\left(\frac{\mu_t}{\sigma_\varepsilon} + \mu \right) \frac{\partial\varepsilon}{\partial x_j} \right] + C_1 \frac{\varepsilon}{k} G - C_2 \bar{\rho} \frac{\varepsilon^2}{k} - C_3 \frac{\varepsilon}{k} \frac{\mu_t}{\bar{\rho}^2} \frac{\partial\bar{\rho}}{\partial x_j} \frac{\partial\bar{p}}{\partial x_j} \quad (7)$$

where the eddy viscosity μ_t is given by

$$\mu_t = C_\mu \bar{\rho} \frac{k^2}{\varepsilon} \quad (8)$$

Standard values were used for all the constants of the model.²⁴ The generation of turbulent kinetic energy, G , is defined as

$$G = -\bar{\rho}\tilde{u}_i''\tilde{u}_j'' \frac{\partial\tilde{u}_i}{\partial x_j} \quad (9)$$

The combustion model

Combustion was modelled assuming a simple chemically reacting system (SCRS). This model is based on the assumption that the reaction rates associated with the fuel oxidation have very small time scales compared with those characteristic of the transport phenomena. Chemical reactions take place instantaneously as soon as the reactants are brought together. Under this assumption, the instantaneous thermochemical state of the gaseous mixture can be determined as a function of strictly conserved scalars. Another common assumption is the equality between the mass diffusion coefficients of all chemical species and the thermal diffusion. If, in addition, the system is adiabatic then all the strictly conserved variables are linearly related. Hence, knowledge of one of

them is sufficient to define the instantaneous thermochemical state of the gaseous mixture. Mixture fraction was the scalar variable chosen for this purpose. The transport equation (3) is solved for mixture fraction with the source term set equal to zero.

In the SCRS model it is further assumed that reaction between the fuel and the oxidant can be represented by a global one-step reaction. This hypothesis allows the calculation of the instantaneous mass fraction of the chemical species as a function of the mixture fraction. If the system in the analysis were adiabatic, instantaneous values of enthalpy and mixture fraction would be linearly related. However, this is not the case for utility boilers. Therefore, an additional assumption about that relationship is needed. The piecewise linear relation suggested in Reference 25 was employed. The temperature can be determined from the enthalpy using well-known thermodynamics relations and density is obtained from the ideal-gas equation of state.

In a turbulent flow, the mixture fraction fluctuates and knowledge of its mean value is insufficient to allow the calculation of the mean values of chemical species mass fractions, temperature and density. The fluctuating nature of the reactive flow may be accommodated through an assumed probability density function (pdf) for the mixture fraction. A clipped Gaussian distribution was assumed in this work. This pdf is completely defined by the mean value and variance of the mixture fraction. The following modelled transport equation for the variance of mixture fraction was solved:

$$\frac{\partial}{\partial x_j} (\bar{\rho} \tilde{u}_j \tilde{f}''^2) = \frac{\partial}{\partial x_j} \left(\frac{\mu_t}{\sigma_g} \frac{\partial \tilde{f}''^2}{\partial x_j} \right) + C_{g1} \mu_t \left(\frac{\partial \tilde{f}}{\partial x_j} \right)^2 - C_{g2} \bar{\rho} \frac{\varepsilon}{k} \tilde{f}''^2 \quad (10)$$

Standard values were assigned to the constants, $C_{g1} = 2.8$ and $C_{g2} = 2.0$

The Favre-average and Reynolds-average values of chemical species mass fractions and temperature are calculated as follows:

$$\tilde{\phi} = \int_0^1 \phi(f) p(f) df \quad (11)$$

$$\bar{\phi} = \bar{\rho} \int_0^1 \frac{\phi(f)}{\rho(f)} p(f) df \quad (12)$$

where the mean density is given by

$$\bar{\rho} = \frac{1}{\int_0^1 \frac{p(f)}{\rho(f)} df} \quad (13)$$

The radiation model

The radiative heat transfer is calculated using the discrete transfer method.²⁶ This method is based on the direct solution of the radiation intensity transport equation. If the participating medium is assumed to be grey and the scattering coefficient is negligible, that equation can be written as

$$\frac{dI}{ds} = -\kappa I + \frac{\kappa \sigma T_g^4}{\pi} \quad (14)$$

The physical domain is divided into several control volumes and the temperature and absorption coefficient are taken as constant in each one. For each control volume adjacent to the boundary,

the central point of the boundary cell is determined. The semihemisphere around that central point is discretized in solid angles. These solid angles define the directions along which equation (14) is integrated.

The total radiative heat flux for each cell on the boundary is calculated from the summation of the radiative intensity of all the radiation beams arriving at that cell. The variation of the radiative intensity of a radiation beam within a control volume is calculated during the solution of equation (14). This variation represents the gain or loss of energy within the control volume. The summation of the gain or loss of energy for all the radiation beams crossing the control volume yields the source term of the energy conservation equation.

The emissivity model

The absorption coefficient of the medium is required to integrate equation (14). In this work the absorption coefficient was calculated from the emissivity of the medium using the mixed grey and clear gas formulation,²⁷ extended to account for soot. The constants and weighing coefficients determined by Truelove²⁸ were employed. The transport equation was solved for soot mass fraction using a soot formation model²⁹ and a soot oxidation model³⁰ to compute the source term.

Boundary conditions

The velocity, the temperature and the mixture fraction are prescribed at the inlet, whereas the kinetic energy of the turbulence and its dissipation rate are estimated (see, e.g., Reference 20). At the walls, the laws of the wall²⁴ are employed. Although this approach may be questionable in respect of heat transfer in complex recirculating flows, it does not present a serious problem for the present application. In fact, heat transfer to the walls in utility boilers is mainly due to radiation and the convective heat transfer has only a minor contribution. The temperature of the walls was assumed to be constant and equal to 700 K. At the exit, a zero gradient normal to the boundary is assumed for the dependent variables. The vertical velocity is then corrected to ensure mass conservation.

3. NUMERICAL MODEL

Discretization of the governing equations

All the Eulerian partial differential equations governing conservation of mass, momentum and energy can be written (in Cartesian co-ordinates) in the following general form:

$$\frac{\partial(\rho u_j \phi)}{\partial x_j} = \frac{\partial}{\partial x_j} \left(\Gamma_\phi \frac{\partial \phi}{\partial x_j} \right) + S_\phi \quad (15)$$

where Γ_ϕ is the diffusion coefficient of the transported variable ϕ . For the particular case of the mass conservation equation, variable ϕ is set equal to one and the right-hand side of the equation is zero.

The governing equations are discretized over a staggered grid using the finite volume/finite differences method. The equations are integrated over each control volume in the computational domain and the Gauss divergence theorem is applied. In the discretization procedure, the fluxes through the boundaries of each control volume must be related with the nodal values. The diffusive terms are discretized using central differences and the convective terms are discretized

using the hybrid upwind/central differences scheme. The discretized equations can be cast in the following form:

$$a_P \phi_P = \sum_i a_i \phi_i + b \quad (16)$$

where the index i runs over all neighbouring points of central grid node P , b denotes the source term and the coefficients a_i and a_P are combined convection/diffusion fluxes across the faces of the control volume (see Reference 31 for details).

The discretization procedure is not affected by the domain decomposition technique. The interblock boundaries behave as a different kind of boundary and the treatment required is described below.

Grid and data structures

The physical domain is divided into a given number of zones. Adjacent zones are overlapped in a small region designated hereafter as an overlapping region (see Figure 1). In this work, only simply overlapped configurations are considered. This means that regardless of the number of zones considered, overlapping regions may only involve two zones. This assumption simplifies the transfer of data between adjacent zones. It could be relaxed at the expense of a more elaborate interface treatment.

Cartesian co-ordinates and a staggered variable arrangement are used in each zone. Adjacent zones have almost independent grids with a single restriction related to the overlapping region. The overlapping region must contain one, and only one, layer of control volumes of scalar variables from each one of the adjacent zones. This is illustrated in Figure 1. In the overlapping region, the control volumes for scalar variables have the same dimension along z direction for

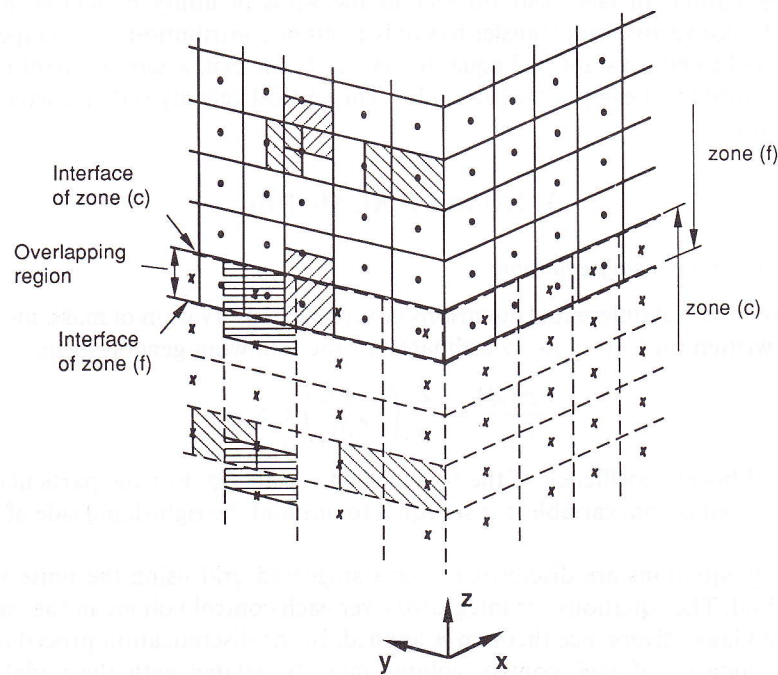


Figure 1. Overlapping region between two zones

both adjacent zones. However, the control volumes of zone (c) are independent from those of zone (f) along directions x and y . Therefore, the adjacent grids are generally discontinuous in the overlapping region.

Domain decomposition does not extend to the calculation of the radiative heat transfer. An independent global grid is used for this calculation.

In each iteration of the solution algorithm, each zone of the domain is treated sequentially. Therefore, the subroutines for the calculation of the coefficients of the discretized equations, the insertion of the boundary conditions and the solution of the sets of discretized equations should be independent of the zone considered. Hence, the dependent variables for all the zones are stored sequentially in one-dimensional arrays.

A three-dimensional array is used to identify the kind of boundary condition (inlet, outlet, wall, symmetry plane or overlapping region) for each boundary cell in each zone. The first index of this array identifies the zone and the orientation of the cell face (north, south, east, west, up or down). The last two indices locate the boundary cell on the boundary zone. The fluxes across the interfaces of each zone are also stored in three-dimensional arrays whose indices are similar to those just described.

Treatment of the interfaces

The solution of the governing equations for each zone requires previous knowledge of the fluxes across the overlapping regions of the zone considered. Continuity of the dependent variables and flux conservation should be ensured across the interfaces. The global fluxes conservation is satisfied by requiring that

$$\sum_i \sum_j F_{i,j}^{(c)} = \sum_l \sum_m F_{l,m}^{(f)} \quad (17)$$

where the indices extend over all the control volumes in the overlapping region between zones (c) and (f).

In this work, an integration procedure is used to transfer data from one zone to the other and an interpolation method is employed to transfer data reversely. Similar techniques have been used by others.^{8,13,32} For illustrative purposes, the overlapping region shown in Figure 1 and the correspondent interface of zone (c) sketched in Figure 2 are considered (co-ordinates are denoted by x and y rather than x_1 and x_2 to avoid a notation with too many subscripts). To solve the governing equations in zone (c), the fluxes across the north interface, $F_{i,j}^{(c)}$ must be known. These fluxes are calculated from the fluxes $F_{l,m}^{(f)}$. The fluxes $F_{l,m}^{(f)}$ are obtained during the solution of the equations in zone (f) using the values of the dependent variables calculated for planes $k = 1$ and $k = 2$ of zone (f). The fluxes $F_{l,m}^{(f)}$ are constant in each boundary cell of zone (f). Calculation of $F_{i,j}^{(c)}$ involves an integration of $F_{l,m}^{(f)}$ across the interface of the zone (c), yielding

$$F_{i,j}^{(c)} = \sum_l \sum_m f_{i,j,l,m} F_{l,m}^{(f)} \quad (18)$$

$f_{i,j,l,m}$ is a weighing factor equal to the fraction of the area of cell (l, m) of zone (f) lying within the cell (i, j) of zone (c). These grid cell faces of zones (f) and (c), shown in Figure 2, coincide on the z -plane interface. The weighing factor is given as follows:

for $x_{i+1/2}^{(f)} \leq x_{i-1/2}^{(c)}$ or $x_{i-1/2}^{(f)} \geq x_{i+1/2}^{(c)}$

$$f_{i,j,l,m} = 0 \quad (19a)$$

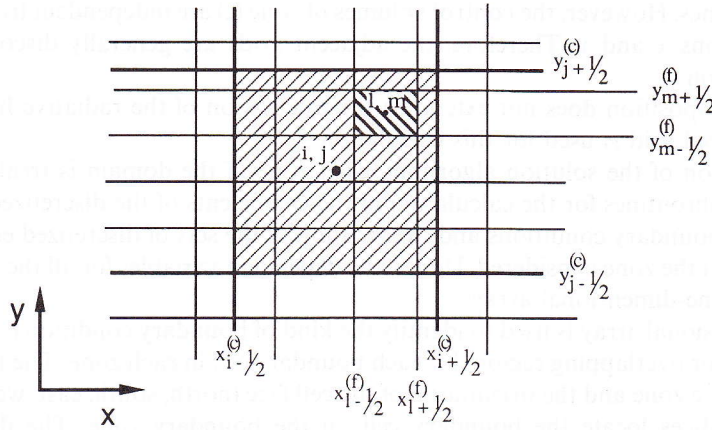


Figure 2. Control volumes at an interface

for $y_{m+1/2}^{(f)} \leq y_{j-1/2}^{(c)}$ or $y_{m-1/2}^{(f)} \geq y_{j+1/2}^{(c)}$,

$$f_{i,j,l,m} = 0 \tag{19b}$$

otherwise,

$$f_{i,j,l,m} = [\min(x_{i+1/2}^{(c)}, x_{i+1/2}^{(f)}) - \max(x_{i-1/2}^{(c)}, x_{i-1/2}^{(f)})] * [\min(y_{j+1/2}^{(c)}, y_{m+1/2}^{(f)}) - \max(y_{j-1/2}^{(c)}, y_{m-1/2}^{(f)})] / [(x_{i+1/2}^{(f)} - x_{i-1/2}^{(f)}) * (y_{m+1/2}^{(f)} - y_{m-1/2}^{(f)})] \tag{19c}$$

Similar expressions may be written for interfaces along planes defined by directions (x, z) or (y, z) .

Now suppose that Figure 2 represents the interface of zone (f). During the solution of the governing equations in zone (c), the fluxes $F_{i,j}^{(c)}$ across the interface of zone (f) were computed from the values of the dependent variables at the planes $k = k_{\max}$ and $k = k_{\max} - 1$ (see Figure 1). A bilinear interpolation method is used to calculate $F_{i,m}^{(f)}$ from $F_{i,j}^{(c)}$. This is followed by an adjustment procedure to guarantee global flux conservation. The bilinear interpolation method yields

$$F_{l,m}^{*(f)} = - \left(\frac{x_l^{(f)} - x_i^{(c)}}{x_{i+1}^{(c)} - x_i^{(c)}} F_{i+1,j}^{*(c)} + \frac{x_{i+1}^{(c)} - x_l^{(f)}}{x_{i+1}^{(c)} - x_i^{(c)}} F_{i,j}^{*(c)} \right) \frac{y_{j+1}^{(c)} - y_m^{(f)}}{y_{j+1}^{(c)} - y_j^{(c)}} + \left(\frac{x_l^{(f)} - x_i^{(c)}}{x_{i+1}^{(c)} - x_i^{(c)}} F_{i+1,j+1}^{*(c)} + \frac{x_{i+1}^{(c)} - x_l^{(f)}}{x_{i+1}^{(c)} - x_i^{(c)}} F_{i,j+1}^{*(c)} \right) \frac{y_m^{(f)} - y_j^{(c)}}{y_{j+1}^{(c)} - y_j^{(c)}} \tag{20}$$

where the star denotes a flux per unit area. The adjusted flux is then

$$F_{l,m}^{(f)} = F_{l,m}^{*(f)} (x_{i+1/2}^{(f)} - x_{i-1/2}^{(f)}) (y_{m+1/2}^{(f)} - y_{m-1/2}^{(f)}) \times \frac{\sum_i \sum_j F_{i,j}^{(c)}}{\sum_l \sum_m F_{l,m}^{*(f)} (x_{i+1/2}^{(f)} - x_{i-1/2}^{(f)}) (y_{m+1/2}^{(f)} - y_{m-1/2}^{(f)})} \tag{21}$$

The numerator in this equation gives the total flux for zone (c) and the denominator is equal to the total flux computed from equation (20) for zone (f). The ratio yields a corrective factor ensuring that equation (17) is satisfied.

The control volumes for the velocity component normal to the interfaces are not contained in the overlapping region since we are dealing with staggered grids. This is illustrated in Figure 1.

However, the treatment of the interfaces is not affected. The only difference lies in the calculation of the fluxes that are stored during the treatment of each zone. Considering, for example, zone (c) of Figure 1, the fluxes $F_{i,j}^{(c)}$ are still computed from $F_{i,m}^{(f)}$ using equation (18). The difference lies in the previous calculation $F_{i,m}^{(f)}$ during the treatment of zone (f). For scalar variables and velocity components along x and y direction, fluxes $F_{i,m}^{(f)}$ across the interface of zone (c) are calculated using the values of the dependent variables at planes $k = 1$ and $k = 2$ of zone (f). But the velocity component along z direction is stored at the interface of zone (c). Therefore, it is directly used for the calculation of $F_{i,m}^{(f)}$.

Solution algorithm

The SIMPLE algorithm was adapted to the zonal method described above. It can be summarized as follows:

- (i) Guess a pressure field for the whole domain.
- (ii) Set to one the variable i that identifies the zone under treatment; set to zero the sums of the absolute normalized residuals for every dependent variable.
- (iii) Calculate the fluxes for the overlapping regions of zone i using the treatment of the interfaces described above.
- (iv) Solve the momentum equations for zone i and store the fluxes at the interfaces of overlapping regions.
- (v) Solve the pressure correction equation for zone i and store the fluxes at the interfaces of overlapping regions.
- (vi) Correct the pressure and velocity fields for zone i .
- (vii) Solve the scalar transport equations for zone i and store the fluxes at the interfaces of overlapping regions.
- (viii) Calculate the thermochemical properties of the gaseous mixture for zone i .
- (ix) Update the sums of the absolute normalized residuals for every dependent variable by adding the contribution of zone i .
- (x) If i is lower than the number of zones, increase i by one and return to step (iii); otherwise, proceed to step (xi).
- (xi) Solve the radiative heat transfer equation.
- (xii) Check if the convergence criterion is satisfied. If not, return to step (ii).

The convergence criterion demands the normalized sum of the absolute residuals for every variable over all the control volumes to be less than or equal to a prespecified value. The normalization value is the mass flow rate for the pressure correction equation, the inlet momentum for the momentum equations and the inlet flux for the remaining variables. The sets of algebraic discretized equations are solved using the Gauss-Seidel line-by-line iterative procedure.

4. RESULTS AND DISCUSSION

The modelled boiler

A power station boiler of the Portuguese Electricity Utility was studied in this work. It is a natural circulation drum boiler with a pressurized combustion chamber, parallel passages by the convection zone and preheating. It is prepared for outdoor installation and fuel oil burning, being easily adapted to natural gas and fuel oil/natural gas burning. Vaporization of the fuel is assumed to occur instantaneously. The boiler is fired from three levels of four burners each,

placed on the front wall. A simplified sketch of the boiler is presented in Figure 3. At maximum capacity (771 t/h at 167 bar and 545°C) the fuel mass flow rate is 15.8 kg/s, the air mass flow rate is 238.7 kg/s and the output power is 250 MW.

The present application is restricted to the combustion chamber as shown in Figure 3. Only one-half of the geometry is considered with symmetry boundary conditions prescribed on the symmetry plane. The skew wall in the ash hopper region was discretized and treated in a stepwise fashion by the flow code to fit into the Cartesian grid system employed. This is a standard approach when modelling utility boilers.¹⁻⁷ However, the actual shape of the ash hopper is taken into account as far as the radiation is concerned.

Comparison between the global and zonal treatments

Three zones were considered and the grids used are shown in Figure 4. The finest grid is used in the burners region (zone 1) and coarser grids are employed in the ash hopper region (zone 2) and above the burners level (zone 3). However, for comparison purposes, calculations were firstly performed for a single domain (test case 1). In this case, the refinement level of the grid in zone 1 was extended to cover the whole domain. Secondly, this grid was employed again, but with the domain divided into the three zones described above (test case 2). In this case, there is grid continuity across the interfaces and the total number of grid nodes becomes higher, since control volumes in the overlapping region are treated twice. Finally, calculations were performed (test case 3) using in each zone the grids depicted in Figure 4. A coarser mesh with $10 \times 9 \times 20$ grid nodes was used for the calculation of the radiative heat transfer for all the test cases.

The computed results are summarized in Table I. The calculation of the radiative heat transfer was only performed every ten iterations. Convergence was achieved when the sums of the absolute residuals were less than 2×10^{-3} .

Comparison of the results obtained for test cases 1 and 2 (see Table I) reveals that the convergence rate is not influenced by the domain decomposition method. In fact, the number of iterations for test cases 1 and 2 is about the same. The CPU time increases from case 1 to case

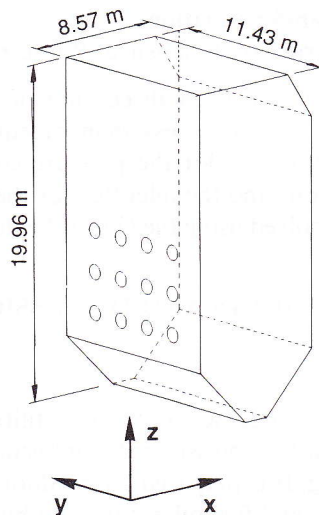


Figure 3. Sketch of the boiler

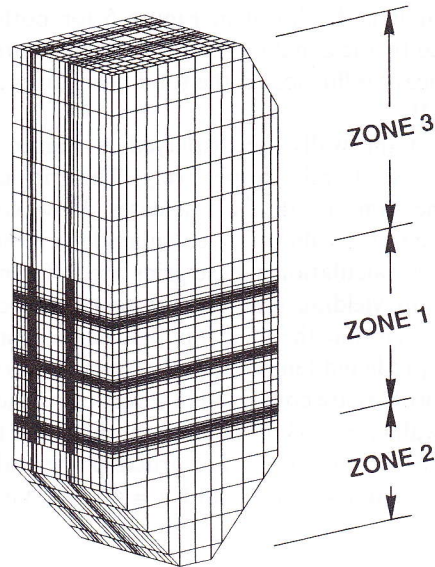


Figure 4. Domain discretization using a zonal method

Table I. Number of iterations and CPU time required for convergence

Test case	Partial number of grid nodes	Total number of grid nodes	Number of iterations	CPU Time (VAX 9000-440)
1	$16 \times 34 \times 60$	30940	902	6 h 45 m
2	Zone 1: $16 \times 34 \times 44$	32028	890	7 h 11 m
	Zone 2: $16 \times 34 \times 8$			
	Zone 3: $16 \times 34 \times 10$			
3	Zone 1: $16 \times 34 \times 44$	27050	779	5 h 34 m
	Zone 2: $10 \times 18 \times 6$			
	Zone 3: $16 \times 18 \times 8$			

2 due to the higher number of grid nodes resultant from the overlapping regions and due to the time required to transfer data between adjacent zones. The total heat fluxes to the walls and the mean values at the exit section are summarized in Table II. They show that the influence of the zonal treatment on those average results is negligible.

Using the domain decomposition presented in Figure 4, the zonal method (test case 3) allows a reduction of 17.5 per cent in the CPU time required to achieve the converged solution compared to the conventional global treatment of the physical domain (test case 1). The number of grid nodes used in test case 1 is only 12.6 per cent smaller than in test case 3. Therefore, significant savings in CPU time can be achieved using the domain decomposition technique. Moreover, the zonal method allows much better resolution of small scale processes to be achieved using a given number of grid nodes due to the better distribution of grid nodes within the physical domain. In a case in which physical scale varies by orders of magnitude, a single grid is not adequate and the use of a multiblock grid is highly recommended.

The evolution of the residuals is displayed in Figure 5 for both cases. It confirms that the convergence rate is not affected by the zonal method employed. Moreover, the zonal treatment of the flow domain has no significant influence on the total heat fluxes at the walls and mean values at the exit section (see Table II).

The predicted heat fluxes at the walls are displayed in Figure 6 for the global and zonal treatments of the domain (test cases 1 and 3, respectively). The grids used for the calculation of the radiative heat transfer are the same in all the test cases. However, the gas temperature and absorption coefficient in each control volume are calculated from the values computed using the finer grids employed in the flow calculation. These grids are different according to the global or zonal treatments of the domain yielding different gas temperature and absorption coefficient fields. Nevertheless, it can be seen that the heat flux distributions are very similar.

Selected vertical profiles of predicted temperature, mixture fraction and oxygen mass fraction are shown in Figure 7. Some profiles are contained in a vertical plane passing through the axes of the burners close to the side wall ($y = 2.43$ m) at different distances from the front wall ($x = 2$ m and $x = 4$ m). The other profiles are contained in a vertical plane midway between vertical planes crossing the axes of the burners at $y = 2.43$ m and $y = 4.62$ m. Very good agreement is found

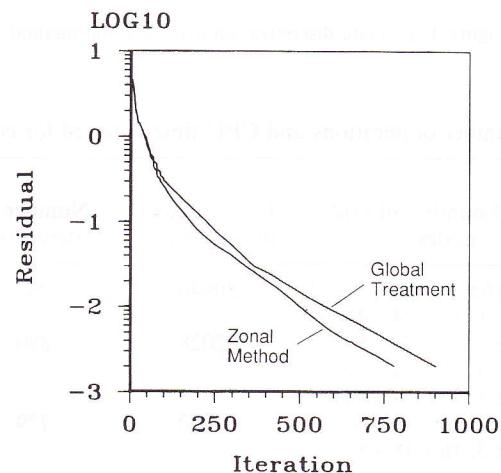


Figure 5. Convergence rate for the global treatment of the physical domain (test case 1) and zonal method (test case 3)

Table II. Predicted total heat fluxes to the walls and mean values at the exit section

Test case		1	2	3
Total radiative heat fluxes (MW)	Front wall	24.9	24.8	24.5
	Side wall	47.7	47.6	47.2
	Back wall	32.4	32.2	32.0
	Ash hopper	15.9	16.0	15.3
Mean values at the exit section	Velocity (m/s)	14.1	14.1	14.2
	Temperature (K)	1556	1551	1561
	Mixture fraction	0.060	0.060	0.060
	Oxygen mass fraction	0.031	0.031	0.031
	Fuel mass fraction	5.7×10^{-6}	5.7×10^{-6}	6.7×10^{-6}

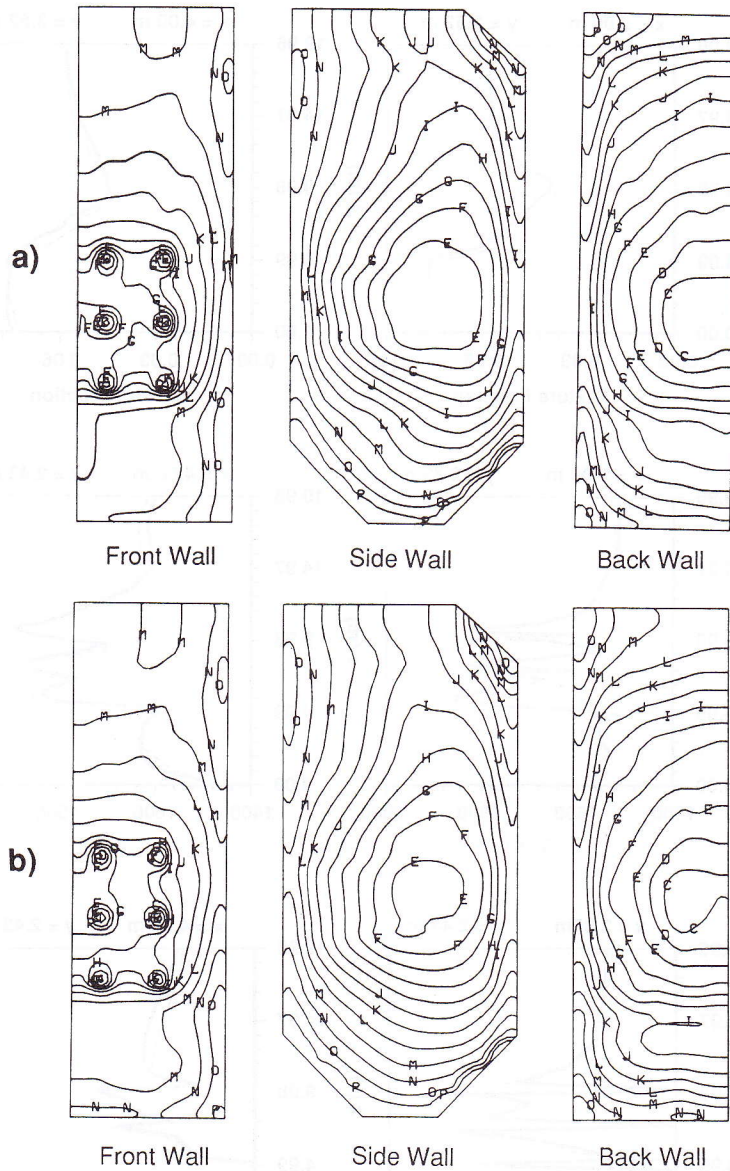


Figure 6. Predicted heat fluxes to the walls, kW m^{-2} (A-525, B-500, C-475, D-450, E-425, F-400, G-375, H-350, I-325, J-300, K-275, L-250, M-225, N-200, O-175, P-150) : (a) Global treatment; (b) Zonal method

between the profiles obtained for global and zonal treatments of the domain. The small differences observed may be attributed to the different grid refinement in each zone.

Continuity of the dependent variables across the interfaces

The results presented so far show that the convergence rate is not influenced by the zonal method employed and the solution obtained is similar to the one computed using a conventional

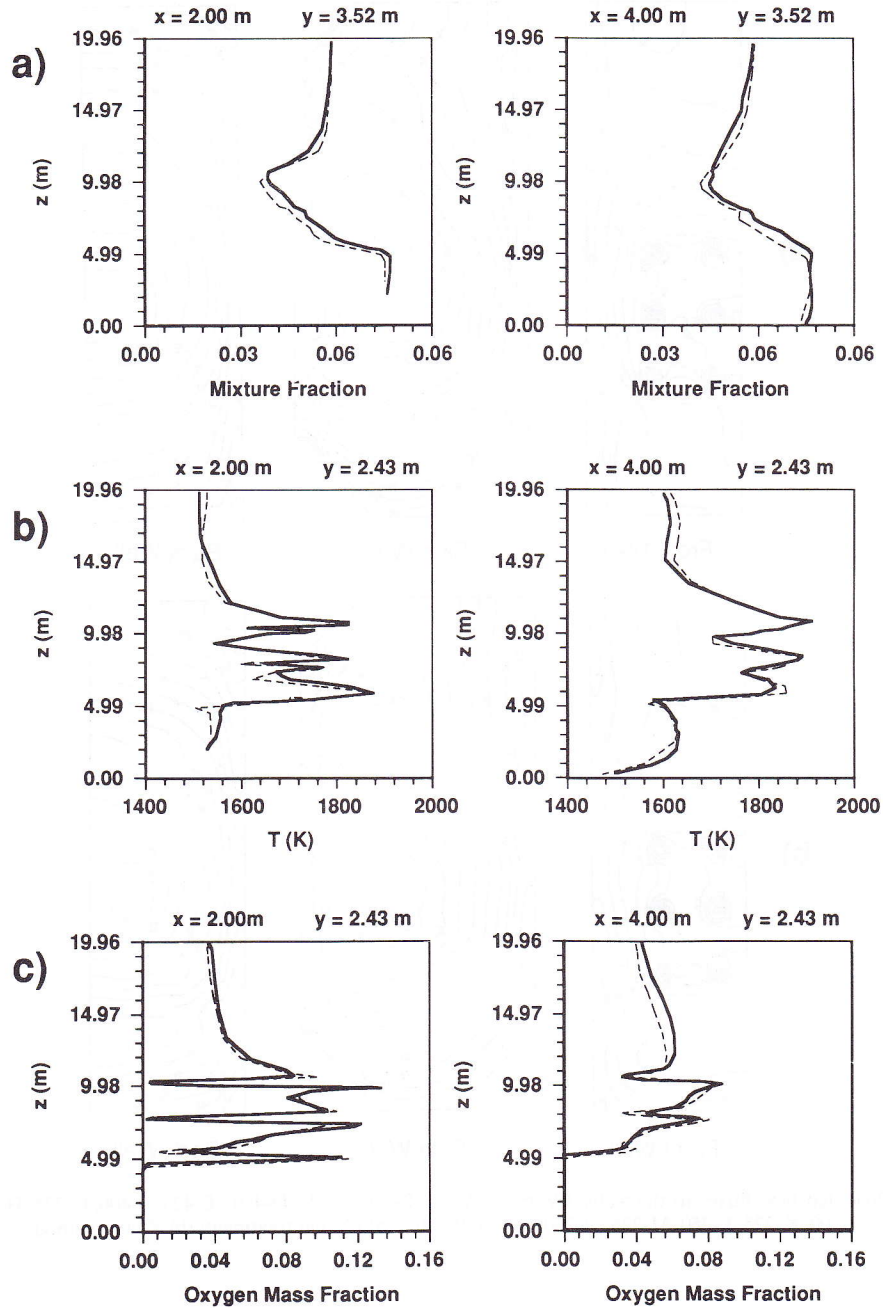


Figure 7. Predicted profiles of temperature (K), mixture fraction and oxygen mass fraction; solid line: global treatment of the domain, test case 1; broken line: zonal method, test case 3

method with no domain decomposition. Now, continuity of the dependent variables across the interfaces will be examined. Only the results computed using the zonal method (test case 3) are considered below.

Figure 8 shows temperature and fuel mass fraction distributions for two vertical planes passing through the axes of the burners ($y = 2.43$ m). The contours were plotted independently for each

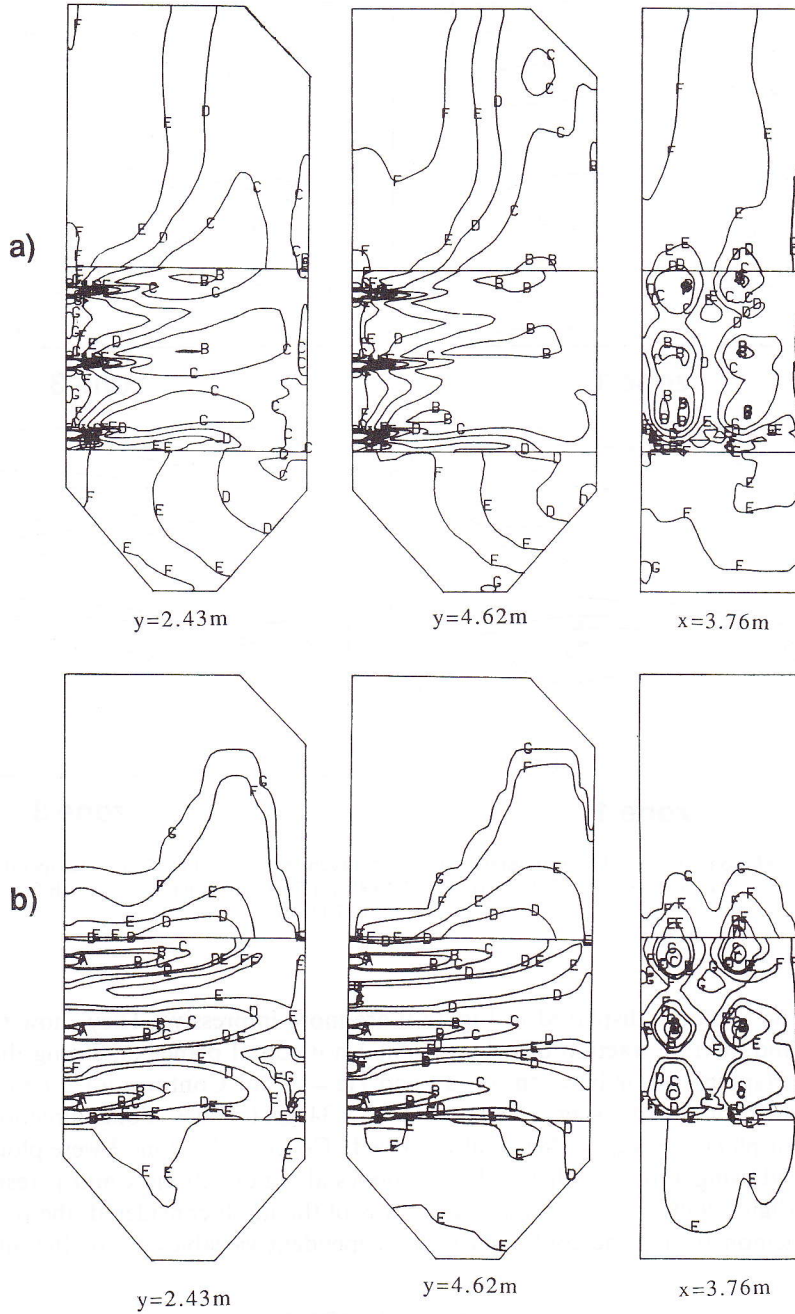


Figure 8. Predicted contours using the zonal method: (a) Temperature, K (A-2000, B-1900, C-1800, D-1700, E-1600, F-1500, G-1400, H-1200, I-1000); (b) Fuel mass fraction (A-0.50, B-0.10, C-0.05, D-0.01, E-0.005, F-0.001, G-0.0001)

one of the zones using the respective predicted results. So, discontinuities across the interfaces can be only due either to the discontinuities of the dependent variables or to the interpolation errors of the plotting routines. The discontinuities of the contours across the interfaces are rather small. Therefore, the zonal method does not seem to affect the continuity of the dependent variables across the interfaces.

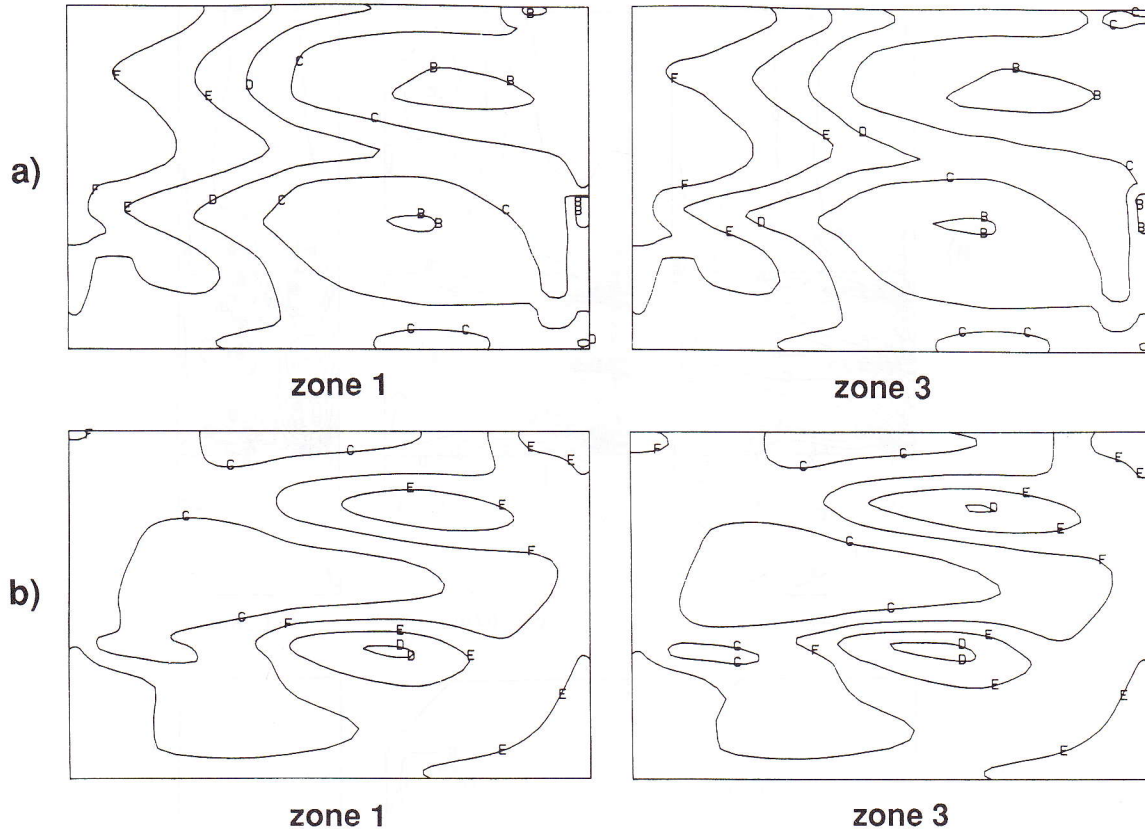


Figure 9. Predicted contours in the overlapping region between zones 1 and 3: (a) Temperature, K (A-2000, B-1900, C-1800, D-1700, E-1600, F-1500, G-1400, H-1200, I-1000); (b) Fuel mass fraction (A-0.25, B-0.15, C-0.10, D-0.08, E-0.07, F-0.06, G-0.05, H-0.04)

However, the contours displayed in Figure 9 are more impressive. They show the predicted temperature and mixture fraction distributions in a horizontal plane containing the grid nodes within the overlapping region between zones 1 and 3 ($z = 11$ m). Contours for zone 1 were plotted from the results computed using a mesh with 16×34 grid nodes along directions x and y , respectively, for plane $k = k_{\max} = 44$ (see also Table I). Contours for zone 3 were plotted from the results obtained using a mesh with 16×18 grid nodes along directions x and y , respectively, for plane $k = 1$. Figure 9 clearly shows that, regardless of the mesh considered, the predictions are very similar demonstrating the continuity of the dependent variables across the interfaces.

5. CONCLUSIONS

In this paper a conservative zonal method was applied to the mathematical modelling of a power station boiler of the Portuguese Electricity Utility. The zonal method was evaluated by performing the following analysis:

- (a) Discretization of the physical domain using a single grid and comparison between the results calculated for two cases:

- (i) global treatment of the domain (test case 1) and
 - (ii) zonal method with three zones continuous across the interfaces (test case 2).
- (b) Discretization of the physical domain using three zones discontinuous across the interfaces and comparison between the results computed for two cases:
- (i) zonal method applied to this domain discretization (test case 3) and
 - (ii) global treatment of the domain considered previously (test case 1).
- (c) Analysis of the continuity of the dependent variables across the interfaces for test case 3 in which a zonal method with discontinuous grids across the interfaces was employed.

The following conclusions may be drawn from the analysis carried out:

- (1) The influence of the domain decomposition procedure on the convergence rate of the solution algorithm is negligible.
- (2) There is a small overhead in CPU time due to data transfer between adjacent zones. However, the zonal method allows grid refinement to be confined to small regions. There is a better distribution of grid nodes within the domain and a reduction in the total number of grid nodes can be achieved. This largely compensates the data transfer overhead. Globally, substantial reductions in CPU time are feasible.
- (3) Owing to the better distribution of grid nodes within the physical domain, the zonal method allows much better resolution of small-scale processes to be achieved using a given number of grid nodes.
- (4) The zonal method does not influence the accuracy of the predicted results.
- (5) There is continuity of the dependent variables across the interfaces.

In this paper, attention was focused on the validation of the domain decomposition procedure. This is better accomplished with a small number of zones and, therefore, only three zones were employed. However, it is anticipated that a much more impressive reduction in CPU time should be achieved by increasing the number of zones since this would allow grid refinement to be confined to the burners region. This is the subject of future research.

NOMENCLATURE

a_i, a_p	combined convection/diffusion coefficients of the discretized equation at nodes i and P , respectively.
b	source term of the discretized equation
C_1, C_2, C_μ	constants of the $k-\epsilon$ turbulence model
C_{g1}, C_{g2}	constants of the modelled transport equation of the mixture fraction variance
f	mixture fraction
f''^2	variance of mixture fraction
$f_{i,j,l,m}$	fraction of control volume (l, m) contained within control volume (i, j)— see Figure 2
$F_{i,j}$	flux across the cell face of control volume (i, j)
G	generation of turbulent kinetic energy
I	radiation intensity
k	turbulent kinetic energy
p	pressure
$p(f)$	probability density function
s	direction of propagation of a radiation beam

S_ϕ	source term of the discretized ϕ -equation
T	temperature
u_i	velocity component along i direction
x_i	Cartesian co-ordinate in i direction

Greek symbols

Γ_ϕ	diffusion coefficient of variable ϕ
δ_{ij}	Kronecker tensor
ε	dissipation rate of turbulent kinetic energy
κ	absorption coefficient
μ	dynamic viscosity
ρ	density
σ	Stefan-Boltzmann's constant
$\sigma_k, \sigma_\varepsilon$	constants of the k - ε turbulence model
σ_ϕ	Prandtl-Schmidt number of variable ϕ
ϕ	dependent variable in a transport equation

Subscripts

g	gas
i	spatial direction
t	turbulent
ϕ	dependent variable

Superscripts

(c), (f)	identification of a zone
-	Reynolds-average value
~	Favre-average value
"	fluctuation quantity in Favre-averaging
*	identification of a flux per unit area

REFERENCES

1. G. F. Robinson, 'A three-dimensional analytical model of a large tangentially fired furnace', *J. Inst. Energy*, 116-150 (1985).
2. A. S. Abbas and F. C. Lockwood, 'Prediction of power station combustors', in *Proc. 21st Symposium (Int.) on Combustion*, The Combustion Institute, 1986, pp. 285-292.
3. R. K. Boyd and J. H. Kent, 'Three-dimensional furnace computer modelling', in *Proc. 21st Symposium (Int.) on Combustion*, The Combustion Institute, 1986, pp. 265-274.
4. K. Görner and W. Zinser, 'Predictions of three-dimensional flows in utility boiler furnaces and comparison with experiments', ASME, 107th Annual Meeting, 7-12 December, Anaheim, California, USA, 1986.
5. W. A. Fiveland and R. A. Wessel, 'Numerical model for predicting performance of three-dimensional pulverized-fuel fired furnaces', *ASME J. Eng. Gas Turbines Power*, **110**, 117-126 (1988).
6. M. G. Carvalho and P. J. Coelho, 'Numerical prediction of an oil-fired water-tube boiler', *Eng. Comput.—Int. J. Comput. Aided Eng. Software*, **7**(3), 227-234 (1990).
7. P. A. Gillis and P. J. Smith, 'An evaluation of three-dimensional computational combustion and fluid-dynamics for industrial furnaces geometries', in *Proceed. 23rd Symposium (Int.) on Combustion*, The Combustion Institute, 1990, pp. 981-991.
8. M. M. Rai, 'A conservative treatment of zonal boundaries for Euler equation calculations', *J. Comput. Phys.*, **62**, 472-503 (1986).
9. Ü. Kaynak and J. Flores, 'Advances in the computation of transonic separated flows over finite wings', *Comput. Fluids*, **17**, 313-332 (1989).
10. A. D. Burns and I. R. Hawkins, 'The solution of laminar and turbulent flow problems using implicit multi-block software', in C. Taylor, H. Chin and G. Hansy (eds.), *Numerical Methods in Laminar and Turbulent Flow*, Vol. VII, Part 2, Pineridge Press, Swansea, 1991, pp. 1443-1453.
11. M. A. Leschziner and K. P. Dimitriadis, 'Computation of three-dimensional turbulent flow in non-orthogonal junctions by a branch-coupling method', *Comput. Fluids*, **17**, 371-396 (1989).

12. R. L. Meakin and R. L. Street, 'Simulation of environmental flow problems in geometrically complex domains. Part 2: a domain-splitting method', *Comput. Methods Appl. Mech. Eng.*, **68**, 311–331 (1988).
13. C. N. Yung, T. G. Keith and K. J. De Witt, 'Numerical simulation of axisymmetric turbulent flow in combustors and diffusers', *Int. j. numer. methods fluids*, **9**, 167–183 (1989).
14. P. N. Wild, F. Boysan, J. Swithenbank and X. Lu, '3-dimensional gas turbine combustor modelling', AGARD CP-422, Paper 27, 1987.
15. M. Rachner, 'Flow computation in combustion chambers using zonal nonstaggered grids', AGARD CP-510, Paper 37, 1991.
16. J. Zhu and W. Rodi, 'Zonal finite volume computations of incompressible flows', *Comput. Fluids*, **20**, 411–420 (1991).
17. M. M. M. Abou-Ellail, A. D. Gosman, F. C. Lockwood and I. E. A. Megahead, 'The prediction of reaction and heat transfer in three-dimensional combustion chambers', *AIAA/ASME Thermophysics and Heat Transfer Conference*, Palo Alto, 1978.
18. A. D. Gosman, F. C. Lockwood, I. E. A. Megahead and N. G. Shah, 'Prediction of the flow, reaction, and heat transfer in a glass furnace', *J. Inst. Energy*, **6**, 353–260 (1982).
19. A. S. Abbas, F. C. Lockwood and A. P. Salooja, 'The prediction of the combustion and heat transfer performance of an experimental refinery heater', *Combust. Flame*, **58**, 91–101 (1984).
20. M. G. Carvalho, D. F. G. Durão and J. C. F. Pereira, 'Prediction of the flow, reaction and heat transfer in an oxy-fuel glass furnace', *Eng. Comput.—Int. J. Computer Aided Eng. Software*, **4**, 23–34 (1987).
21. M. G. Carvalho, P. Oliveira and V. Semião, 'A three-dimensional modelling of an industrial glass furnace', *J. Institute Energy*, 143–157 (1988).
22. P. J. Coelho and M. G. Carvalho, 'Evaluation of a three-dimensional mathematical model of a power station boiler', submitted to *ASME J. Eng. Gas Turbines Power*.
23. K. K. Kuo, *Principles of Combustion*, Wiley, New York, 1986.
24. B. E. Launder and D. B. Spalding, 'The numerical computation of turbulent flows', *Comput. Methods Appl. Mech. Eng.*, **3**, 269–289 (1974).
25. M. M. M. Abou-Ellail, A. D. Gosman, F. C. Lockwood and I. E. A. Megahead, 'Description and validation of a three-dimensional procedure for combustion chamber flows', *J. Energy*, **2**, 71–80 (1978).
26. F. C. Lockwood and N. G. Shah, 'A New Radiation Solution Method for Incorporation in General Combustion Prediction Procedures', in *Proc. 18th Symposium (Int.) on Combustion*, The Combustion Institute, 1981, pp. 1405–1414.
27. H. C. Hottel and A. F. Sarofim, *Radiative Transfer*, McGraw-Hill, New York, 1967.
28. J. S. Truelove, 'A mixed grey gas model for flame radiation', AERE Harwell, *Report HL76/3448/KE* (1976).
29. I. M. Khan and G. A. Greeves, 'A method for calculating the formation and combustion of soot in diesel engines', in Afgan, Beer (eds.), *Heat Transfer in Flames*, 1974, pp. 391–402.
30. B. F. Magnussen and B. H. Hjertager, 'On Mathematical Modelling of Turbulent Combustion with Special Emphasis on Soot Formation and Combustion', in *Proc. 16th Symposium (Int.) on Combustion*, The Combustion Institute, 1977, pp. 719–728.
31. S. V. Patankar, *Numerical Heat Transfer and Fluid Flow*, Hemisphere, New York, 1980.
32. K. A. Hennesius and M. M. Rai, 'Applications of a conservative zonal scheme to transient and geometrically complex problems', *Comput. Fluids*, **14**, 43–58 (1986).